TRIBOLOGY AND INTERFACE ENGINEERING SERIES, 55
EDITOR: B.J. BRISCOE

TRIBOLOGY OF POLYMERIC NANOCOMPOSITES

Friction and Wear of Bulk Materials and Coatings

Klaus Friedrich
Alois K. Schlarb

Amsterdam • Boston • Heidelberg • London • New York • Oxford
Paris • San Diego • San Francisco • Singapore • Sydney • Tokyo

CHAPTER 11

Wear and wear maps of hard coatings

Dongfeng Diao and Koji Kato

Contents

Abstract

Delamination is the most harmful type of wear of hard coatings in practical use. It is generated even by a single action of indentation of a harder pin into the coating. Cracks of ring, radial and/or lateral types are generated around the contact region of the coating, and partial or general delamination of coating is induced depending on the contact conditions.

When cracks of such types are not generated by static contact under milder contact condition, delamination of coating is generated by repeated sliding as one type of wear in the outside or inside of the wear track. The progressive wear, which takes place at micro-contacts between asperities on the surfaces of coating and pin, reduces the thickness of coating by every sliding cycle and promotes the generation of delamination in the inside of the wear track.

The behavior of such modes of delamination follows the law of low cycle fatigue, where the site of local yield in the coating and substrate becomes important together with the initial distribution of micro defects in the coating and substrate including the coating surface and bonding interface.

Based on this kind of understanding of delamination mechanism, wear maps are introduced to distinguish the region of crack initiation and propagation in relation to the yield strength ratio between the coating and substrate and the ratio of coating thickness/contact radius.

11.1 Introduction

The coating of tribo-element is mainly made to protect the surface of substrate from wear, and a material harder than substrate is generally chosen for the coating[1]. Although there are commonly known wear modes of abrasive, adhesive and corrosive for metals[2], they are all included in the term of "progressive wear" in this chapter and the wear mode of "delamination" is high lighted in the following as the most harmful types of wear of coating by generating flake-like or ribbon-like wear particles[3].

11.2 Delamination of hard coatings by indentation

Fig.11.1 shows the indentation mark and crack pattern as functions of normal load W and coating thickness with three regions [4]. In Fig. 11.1(a), a SiC ball of 1.5 mm radius is indented into the Al_2O_3 coating, and three patterns of no crack, ring crack and partial delamination between ring cracks are observed around the indentation mark. It can be seen from the figure in the thickness range of t = 1~13 μm that an indentation mark without ring cracks[1] (Hertz crack) is observed with the load below W = 500 N and one or two ring cracks are observed with the load W = 800~1900 N. When W is larger than about 2000 N, ring cracks more than three are generated and partial delamination takes place between neighboring rings.

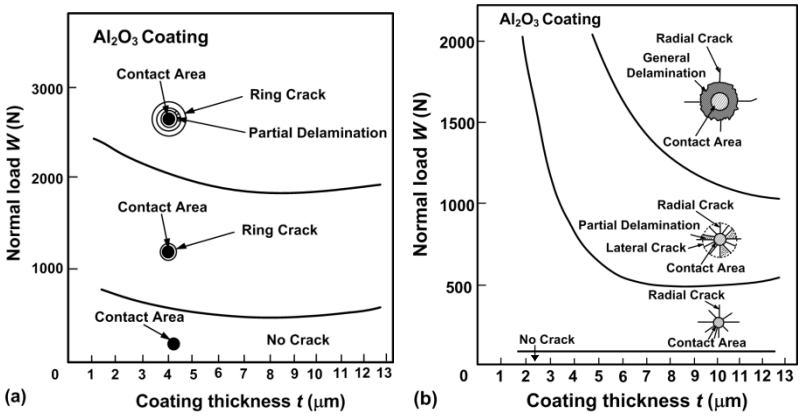

Fig. 11.1. The indentation mark and crack pattern as a function of normal load W and coating thickness t at the surface of Al_2O_3 coating on WC-Co substrate. (a) indentation of a SiC ball of 1.5 mm radius, (b) indentation of a diamond pin of 0.2 mm tip radius[4].

In Fig.11.1(b), a spherical diamond pin of 0.2 mm tip radius is indented into the same Al_2O_3 coating as for Fig. 11.1(a), where the contact pressure is much higher with smaller contact area than that of a SiC ball of 1.5 mm radius under the same load. Observed crack patterns are classified into four types with four regions; the type of no crack, the type of radial cracks[2] only around the indentation mark under relatively small load, the type of radial and lateral cracks together with partial delamination of coating under medium load and the type of general delamination of coating by the general propagation of lateral cracks [3] under relatively large load.

1 The ring crack or Hertz crack is generated in loading process along the periphery of Hertz contact region when the maximum tensile stress there exceeds a critical value of the brittle material with the pre-existent surface cracks and is propagated downward to form a shape of cone. Hertz contact is defined as the elastic contact between balls or a ball and a flat [5].

2 The radial crack is generated in loading process at the central part of plastically deformed zone in the contact region of indenter when the maximum tensile stress there exceeds a critical value of the brittle material and is propagated radially from the center of contact [6].

3 The lateral crack is generated in un-loading process at the central part of the plastically deformed zone in the contact region of indenter when the maximum tensile stress generated by the residual stress there exceeds a critical value of the brittle material, and is propagated in parallel to the surface [7].

The critical load for generating partial delamination of coating in Fig.11.1(b) is almost constant at around W = 500 N for the coating thickness t above 6 μm, however it is increased rapidly if the thickness t is reduced from 6 to 1 μm. The critical load for generating general delamination of coating behaves similarly against the coating thickness at higher level of load.

The critical load W_{HC} for generating a ring or Hertz crack and the critical load W_{LC} for a lateral crack in the coating are described theoretically by D. F. Diao et al [4] as follows;

$$W_{HC} = 200K_{IC,C}^{3}R^{2}E_{eff}^{-2}C^{-3/2} \tag{11.1}$$

$$W_{LC} = 1.4 \times 10^{6}K_{IC,inter}t^{3/2}\left(\frac{H_{eff}}{E_{eff}}\right)^{1/2} \tag{11.2}$$

where $K_{IC,C}$ is the fracture toughness of coating, R the radius of indenter, E_{eff} the effective elastic modulus of coating and substrate, C the length of pre-existent surface crack, $K_{IC,inter}$ the fracture toughness of bonding interface, t the coating thickness and H_{eff} the effective hardness of coating and substrate.

Figure 11.2 shows the agreement between the experimental and theoretical values of W_{HC} for Al_2O_3 coating on WC-Co substrate in the coating thickness range from 1 to 13 μm. Figure 11.3 shows the good agreement between the experimental and theoretical values of W_{LC} for the same coating.

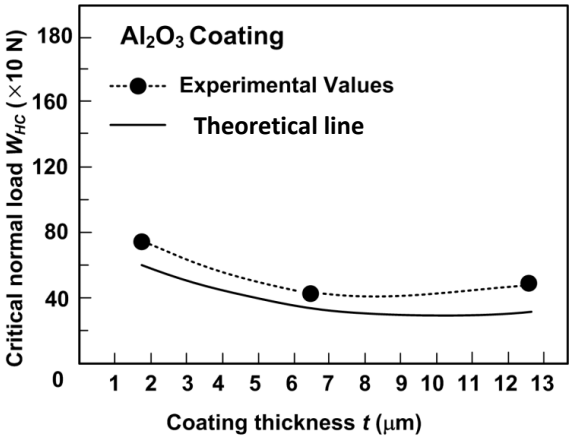

Fig. 11.2. Experimental and theoretical critical loads for ring crack generation in Al_2O_3 coating on WC-Co substrate by indentation of a SiC ball of 1.5 mm radius [4].

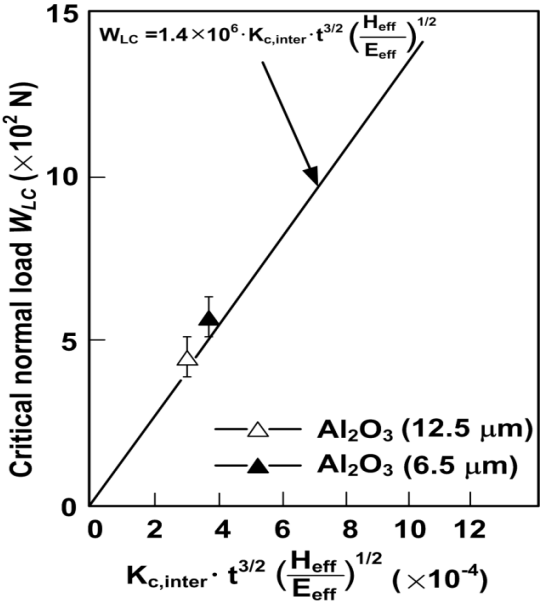

Fig.11.3. Experimental and theoretical critical loads for lateral crack generation in Al_2O_3 coating on WC-Co substrate by indentation of a diamond pin of 0.2 mm tip radius [4].

11.3 Progressive wear and delamination of hard coatings in repeated sliding

In repeated sliding of a diamond pin of 33 μm tip radius against an Al_2O_3 coating of 1.0 μm thickness on WC-Co substrate, only a small amount of plastic deformation of asperities on the coating surface is generated as shown in Figs.11.4(a) and (b) when the contact is mild with a relatively light load(0.1N), where the wear mode is plowing[3]. Fine powder-like wear particles are generated after a certain amount of repeated sliding cycles, as shown in Figs.11.4(c) and (d). A large amount of powder-like wear particles are stacked on the tip-surface and scattered along the wear track after 100 sliding cycles as shown in Figs.11.4(e) and (f).

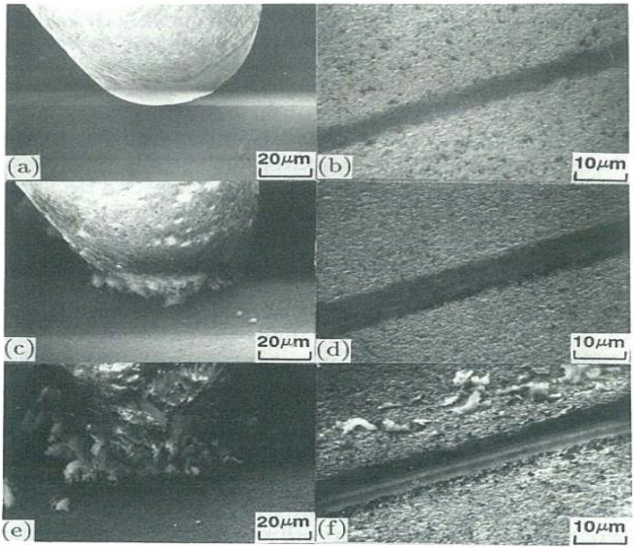

Fig. 11.4. SEM images of progressive wear of Al_2O_3 coating of 1μm thickness observed in repeated sliding of a diamond pin of 33μm tip radius under 0.1N load. (a) and (b); at the 1st cycle, (c) and (d); at the 50th cycle, (e) and (f); at the 100 th cycle [3].

Under more severe contact with a relatively large load(1.5N), cracks are introduced at either or both sides of the wear track, and flake-like wear particles are generated by delamination of coating in the outside of the wear track as shown in Figs. 11.5(a), (b) and (c). After having progressive wear and thinning of coating, long ribbon-like wear particles are generated by delamination of coating in the inside of the wear track as shown in Figs.11.5(d) and (e)[8].

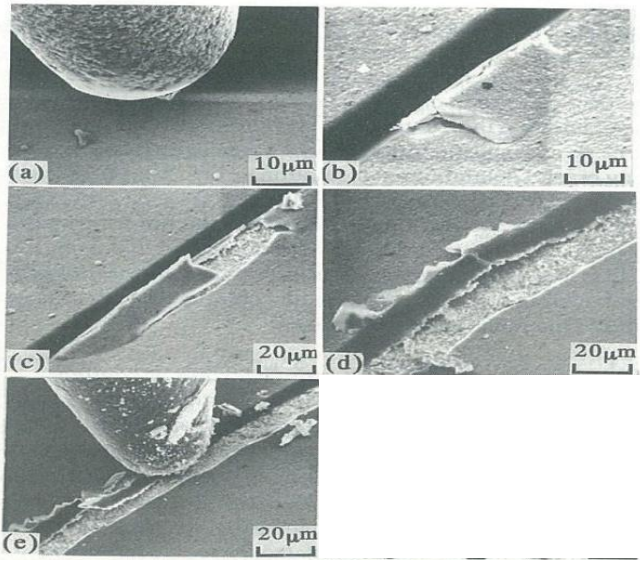

Fig. 11.5. SEM images of delamination of Al_2O_3 coating of 1μm thickness observed in repeated sliding of a diamond pin of 33μm tip radius under 1.5N load. (a); at the 1st cycle, (b); at the 3rd cycle, (c); at the 4^{th} cycle, (d); at the 9^{th} cycle, (e); at the 10^{th} cycle[8].

Under very severe contact with a large load above 1.5 N, cracks are developed far below the surface of wear track and thick flake-like wear particles are generated by delamination. Fig.11.6 shows the magnified view of a flake-like wear particle which shows substrate material bonding to the flake and tells that the crack path was in the substrate[8]. Fig.11.7 shows the regimes of wear modes observed in Figs.11.4 and 11.5 as a function of normal load *W* and the number of sliding cycles *N*. Fig.11.8 gives the values of wear rate (mm^3/Nm) observed in the load range from 0.1 to 1.8N, where the load of 0.1 N only gives the practically acceptable value of w_s below 10^{-6} mm^3/Nm.

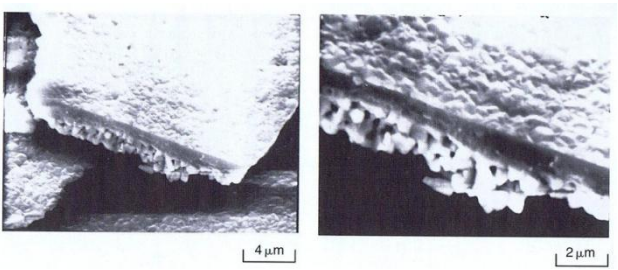

(a) (b)

Fig. 11.6. SEM images of a flake-like wear particle of Al_2O_3 coating delaminated by crack propagation in the substrate. (a) an over view, (b) a side view showing the substrate material[8].

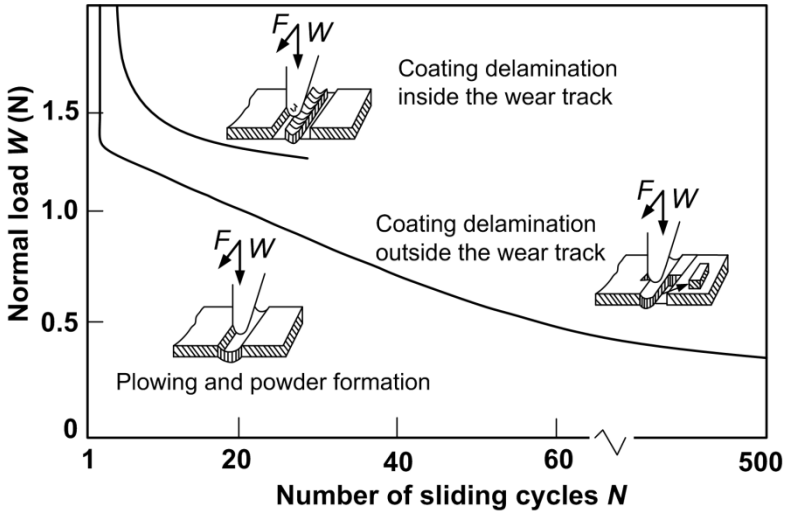

Fig. 11.7. Wear modes of Al_2O_3 coating of 1μm thickness observed in repeated sliding of a diamond pin of 33μm tip radius under various loads and sliding cycles. W; load, F; friction [3].

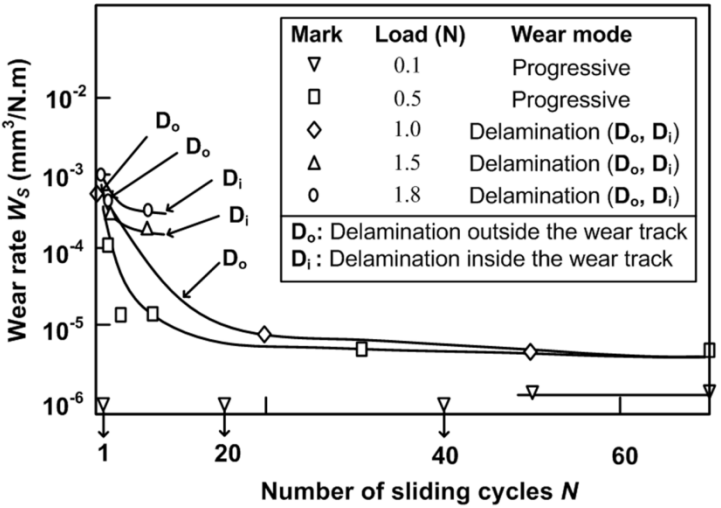

Fig. 11.8. Wear rates and wear modes of Al_2O_3 coating of 1 μm thickness observed in repeated sliding of a diamond pin of 33 μm tip radius under various loads and sliding cycles. ▽ under 0.1N and □ under 0.5 N load; progressive wear, ◇ under 1.0 N load; coating delamination outside the wear track, △ under 1.5 N and ○ under 1.8 N load; coating delamination outside and inside the wear track [3].

The possible mechanism of coating delamination at the outside of the wear track by sliding of a hard pin is considered as illustrated in Fig.11.9 [9]. The pre-existent micro-cracks at the bonding interface are propagated to the vertical direction against sliding in Fig.11.19(a) and a large crack is formed along the bonding interface in Fig.11.19(b) due to the localized plastic deformation in the contact region. The compressive stress σ_c generated by the plastic deformation finally induces delamination of coating as shown in Fig.11.9(c) by releasing the compressive stress. A load, which is large enough to introduce the plastic deformation in the contact region, is therefore necessary for this mechanism.

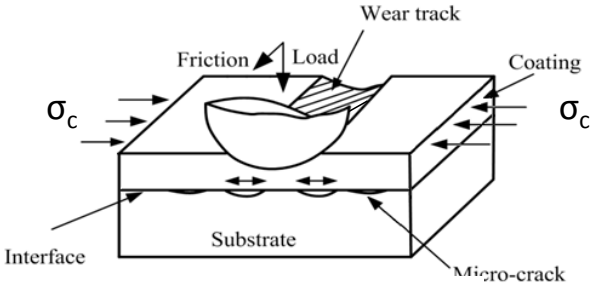

(a) Propagation of micro-cracks

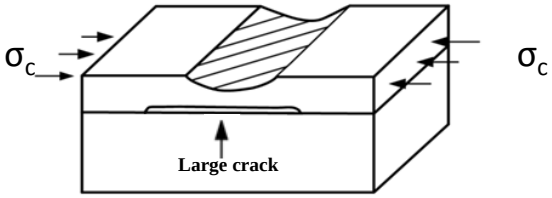

(b) Formation of a large crack

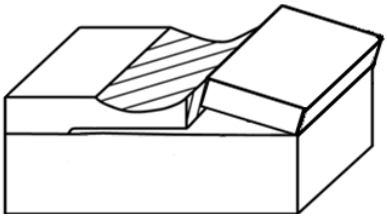

(c) Delamination of coating

Fig. 11.9. A model of delamination of coating at the outside of the wear track induced by the compressive stress σ_c generated by the localized plastic deformation in the contact region. (a); propagation of microcracks, (b); formation of a large crack, (c); delamination of coating.

The possible mechanism of coating delamination at the inside of the wear track by repeated sliding is considered as illustrated in Fig.11.10. The pre-existent micro-cracks at the bonding interface are propagated to the direction of sliding in Fig.11.10(a), and a large crack is formed by repeated sliding along the bonding interface in Fig.11.10(b). When the coating thickness is reduced to a critical value by progressive wear and/or when the large crack is grown to a critical size, delamination of coating is finally induced as shown in Fig.11.10(c) by releasing the residual compressive stress σ_r in the coating.

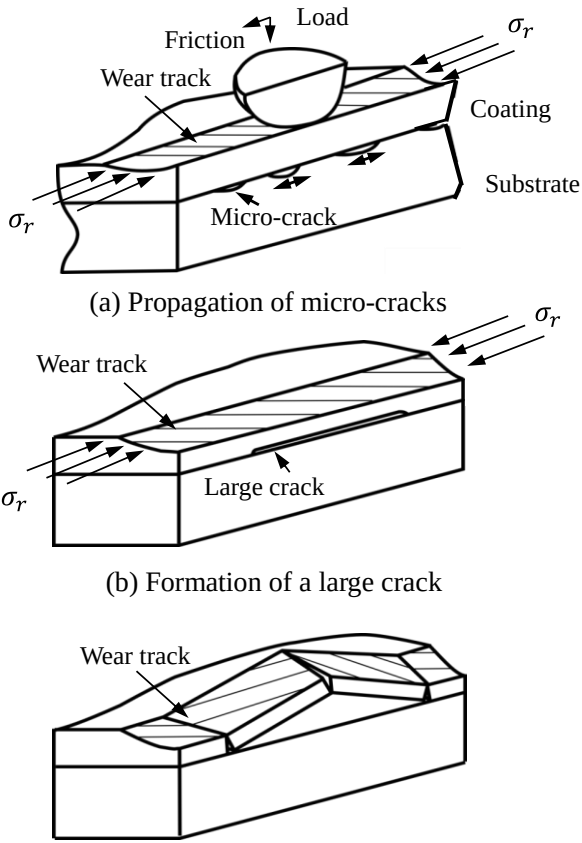

Fig. 11.10. A model of delamination of coating at the inside of the wear track induced by the progressive wear and the residual compressive stress σ_r in the coating. (a); propagation of micro-cracks, (b); formation of a large crack, (c); delamination of coating.

11.4 Low cycle fatigue law of delamination

Fig.11.11 shows the wear track (1μm×1μm) of CN_x coating of 100 nm thickness on Si wafer after 40 transverse repeated sliding cycles by a diamond pin of 150 nm tip radius under 14μN load. The wear track of CN_x coating is formed by wear as shown in Fig.11.12 where the progressive and sudden increase in depth of wear track is described as a function of number of repeated sliding cycles[10]. Similar results are observed in [11,12].

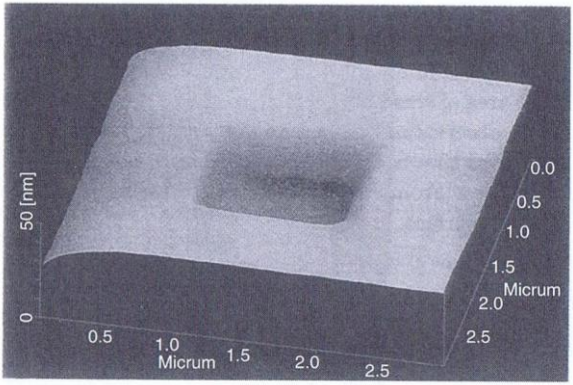

Fig. 11.11. AFM image of wear track of CN_x coating on Si wafer formed by 40 transverse sliding cycles with a diamond pin of 150 nm tip radius[10].

It is clearly shown in the figure that the depth of wear track is drastically increased by the repeated sliding cycle from 13th to 14th and that from 29th and 30th.

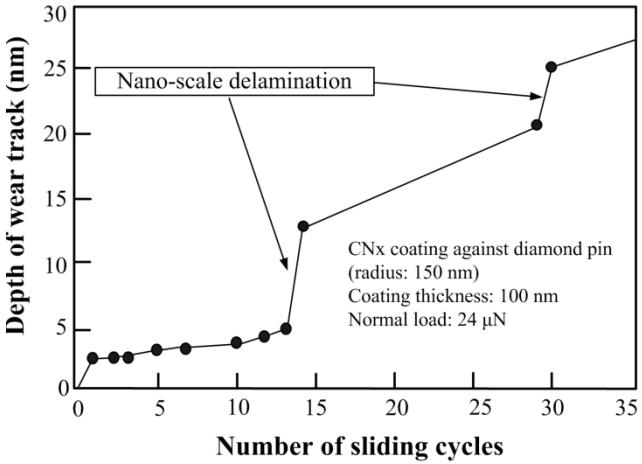

Fig. 11.12. The sudden increase in depth of wear track caused by nano-scale delamination of CN_x coating after progressive wear in repeated sliding with a diamond pin of 150 nm tip radius[10].

This kind of sudden increase in depth of wear track is caused by the sudden delamination of a thin surface layer of the coating in the wear track as shown in Fig. 11.13, where the wavy surface of wear track at the 18th sliding cycle in Fig. 11.13(a) is suddenly disappeared by surface delamination at the 19th sliding cycle in Fig. 11.13 (b). The critical number of sliding cycles for the generation of delamination is decreased by increasing the contact load from 14 to 45 μN as shown in Fig. 11.14.

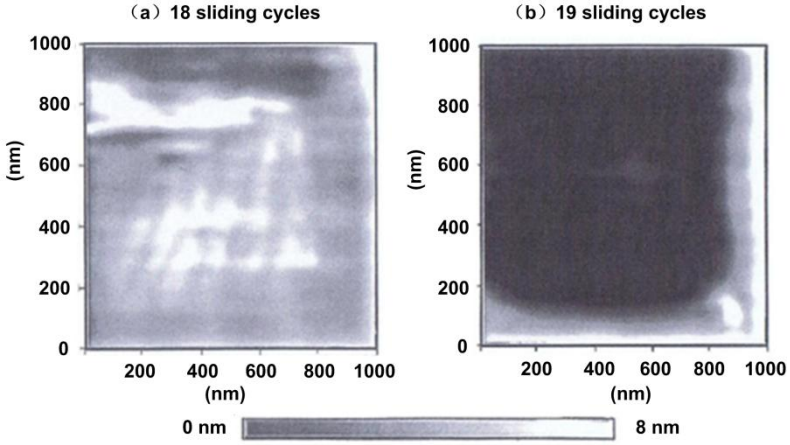

Fig. 11.13. AFM images of wear track of CN_x coating on Si wafer formed by repeated sliding with a diamond pin of 150 nm tip radius. (a); wavy surface of wear track after 18 cycle, (b); dark image of wear track after surface delamination at 19^{th} cycle[10].

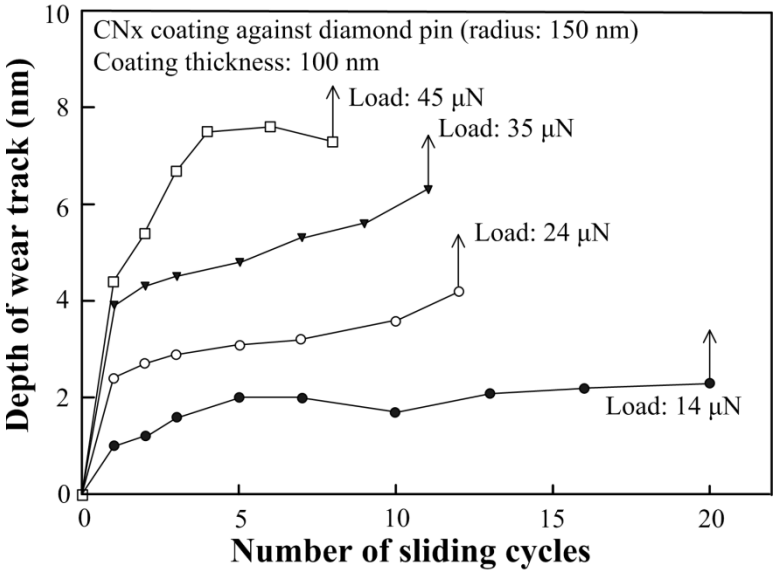

Fig. 11.14. The load dependency of the critical number of sliding cycles for the sudden increase in depth of wear track by surface delamination of CN_x coating of 100 nm thickness on Si wafer by repeated sliding with a diamond pin of 150 nm radius[10].

If a simple model of contact is described as shown in Fig.11.15 where a is the contact radius and R the radius of pin tip, the representative plastic strain $\Delta\varepsilon_p$ at the contact region of the diamond pin is given as follows[13],

$$\Delta\varepsilon_p = 0.18\, a/R \tag{11.3}$$

The value of a is calculated by the following equation,

$$a^2 = R^2 - (R - \Delta h_a)^2 \tag{11.4}$$

where Δh_a is the average increase of wear depth per sliding cycle and is defined as follows,

$$\Delta h_a = \sum_{n=1}^{N_d} \Delta h_n / N_d \tag{11.5}$$

ln Eq(11.5), Δh_n is the increase of wear depth per sliding cycle which is obtained from the depth of wear track in Fig.11.16, and N_d the number of sliding cycle for delamination.

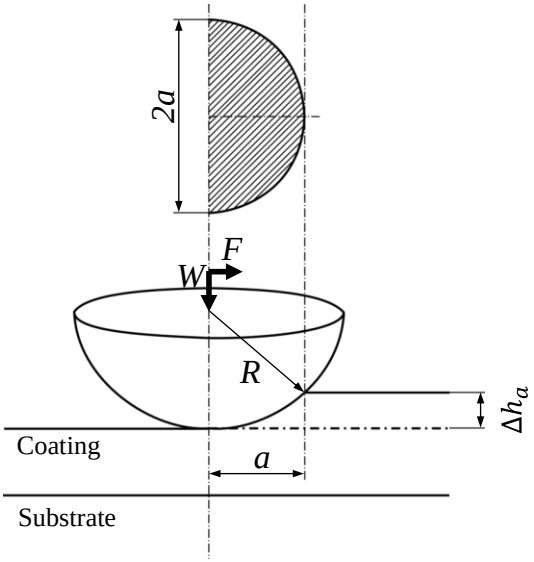

Fig.11.15. Schematic image of sliding contact between the coating and a hard spherical pin. *R*; radius of pin tip, *a*; contact radius, Δh_a; wear track depth at the *n*th sliding cycle, W; load, F; friction.

Figure 11.16 shows the relationship between the experimental values of $\Delta\varepsilon_p$ and N_d obtained by changing the pin radius and contact load[11,12], where it is described by the following equation

$$N_d^{\beta}\Delta\varepsilon_p = c \tag{11.6}$$

and β and c are experimental constants.

The observed relationship of Eq.(11.6) clearly tells that the wear mode of delamination follows the power law of low cycle fatigue proposed by Coffin and Manson[14,15].

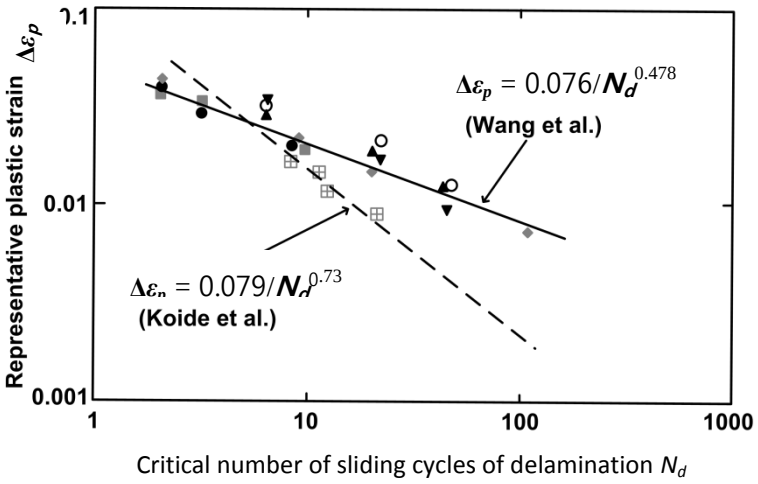

Fig.11.16. The power law observed between the representative plastic strain $\Delta\varepsilon_p$ and the critical friction cycle N_d for surface delamination: the broken line;by the diamond pin of 150 nm tip radius under 15~45 μN load, the solid line;by the diamond pin of 10 μm tip radius under 10~250 μN load[11].

11.5 Wear maps of hard coatings

It is shown in the previous sections of 11.3 and 11.4 that a hard coating of brittle material is worn by delamination under repeated sliding of a hard pin. The thickness of wear particles can be similar to the thickness of coating, or, smaller or larger than that of coating depending on the severity of contact. In any cases, the mechanism of delamination seems low cycle fatigue associated with the repeated plastic strain cycle in the localized zone. Because of this understanding about the mechanism of delamination of coating, the stress distribution of equivalent stress of von Mises, σ_{VM}, on the x-z plane at $y = 0$ in Fig.11.17 is calculated with the semi-analytical method SAM, which is based on the conjugate gradient method and the discrete convolution and the fast Fourier transform technique, for the sliding contact between a ball and the coating of thickness t under the load W and friction F[16].

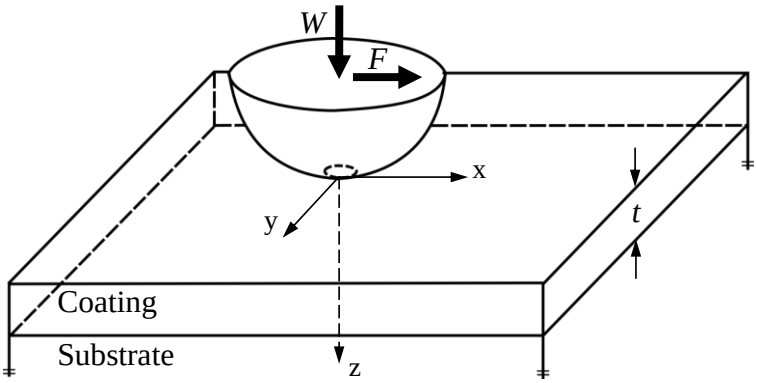

Fig.11.17. The model of sliding contact between a ball and the coating. W; load, F; friction, t; coating thickness.

Fig.11.18 shows the contours of σ_{VM} normalized by the maximum Herzian contact pressure, P_{max} , on the diagram of x/a and z/a where a is the contact radius[16]. The values of σ_{VM}/P_{max} in the figure are for the case of the friction coefficient $\mu = 0.25$ and $E_c/E_b = 2$, where E_c is the elastic modulus of coating and E_b of substance. In Fig.11.18 (a) for $t = 0.125a$, the regions of high value of σ_{VM}/P_{max} are observed on the coating surface, in the coating and in the substance, where the maximum value of $(\sigma_{VM}/P_{max})_{max} = 0.81$ is generated on the coating surface. In Fig.11.18(b) for $t = 0.5a$, the regions of high values of σ_{VM}/P_{max} are observed in the coating and around the bonding interface, where $(\sigma_{VM}/P_{max})_{max} = 1.02$ is generated at the bonding interface. In both Fig.11.18 (c) for $t = a$ and Fig.11.18 (d) for $t = 2a$, the region of highest value of σ_{VM}/P_{max} is generated in the coating, where $(\sigma_{VM}/P_{max})_{max} = 0.93$ in (c) and $(\sigma_{VM}/P_{max})_{max} = 1.00$ in (d).

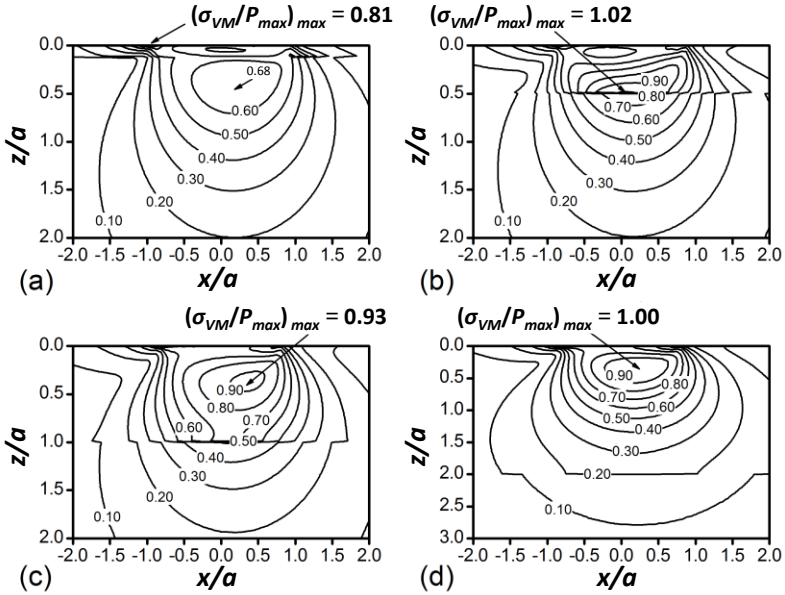

Fig.11.18 Contours of the normalized stress of von Mises stress, σ_{vm}/P_{max}, in the *x*-*z* plane at $y = 0$ for $\mu = 0.25$ and $E_c/E_b = 2$. (a) $t = 0.125a$, (b) $t = 0.5a$, (c) $t = a$, (d) $t = 2a$[16].

Fig.11.19 shows the contours of σ_{VM}/P_{max} obtained for the case of $\mu = 0.5$ and $E_c/E_b = 2$ by the calculation similar to that of Fig.11.18[16]. In Fig.11.19 (a) for $t = 0.125a$, the regions of high value of σ_{VM}/P_{max} are observed on the coating surface and in the coating, where $(\sigma_{VM}/P_{max})_{max} = 1.33$ is generated on the coating surface. In Figs. 11.19 (b) for $t = 0.5\ a$, (c) for $t = a$ and (d) for $t = 2a$, the region of highest value of σ_{VM}/P_{max} is generated on the coating surface, where $(\sigma_{VM}/P_{max})_{max} = 1.34$ in (b), $(\sigma_{VM}/P_{max})_{max} = 1.42$ in (c) and $(\sigma_{VM}/P_{max})_{max} = 1.50$ in (d).

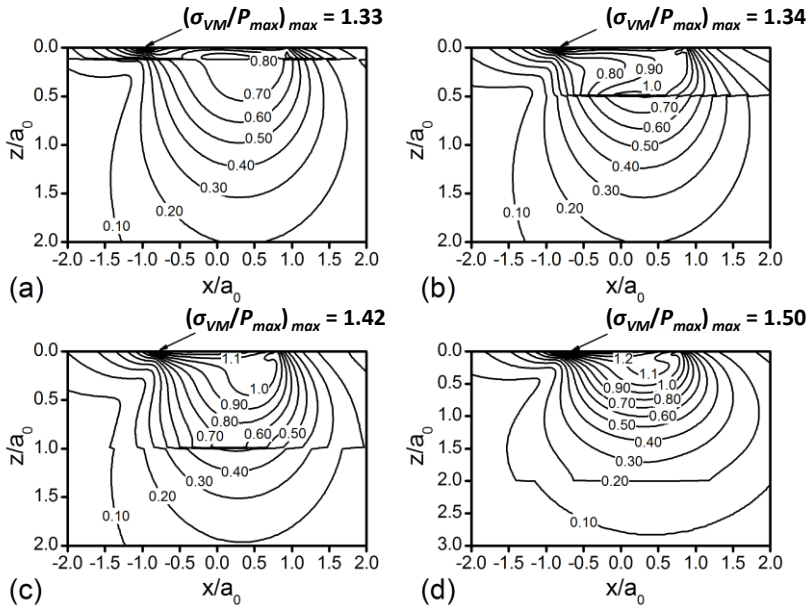

Fig.11.19 Contours of the normalized von Mises stress, σ_{vm}/P_{max}, in the *x*-*z* plane at *y* = 0 for μ = 0.5 and E_c/E_b = 2. (a) t = 0.125a, (b) t = 0.5a, (c) t = a, (d) t = 2a[16].

After having similar distributions of contours of σ_{VM}/P_{max} for μ = 0 and μ = 0.70 in the range from t = 0 to t = 4a, the site of yield initiation, where the maximum value of σ_{VM} exceeds the yield stress of the material, was confirmed in the contact stress region for various combinations of t/a and Y_c/Y_b, where Y_c is the yield strength of coating and Y_b of substrate.

The four regions of Ⅰ, Ⅱ, Ⅲ and Ⅳ, which indicate the sites of local yield initiation in the contact stress region of the coating and substrate, are shown on the diagram of t/a and Y_c/Y_b in Fig.11.20, where the yield strength of the bonding interface is assumed to be the same as that of the substrate and E_c/E_b = 2.0[16].

Fig.11.20 (a) for μ = 0 shows that the yield initiation takes place in the substrate on the region Ⅰ, at the bonding interface on the region Ⅱ and in the coating on the region Ⅲ. Fig11.20 (b) for μ = 0.25 and E_c/E_b = 2.0 shows that the small region Ⅳ appears for the yield initiation on the coating surface in addition to the regions of Ⅰ, Ⅱ and Ⅲ. When the friction coefficient μ is further increased to 0.50 in Fig.11.20 (c) and to 0.70 in Fig.11.20 (d), only two regions are observed: region Ⅲ for the yield initiation at the bonding interface and region Ⅳ for the yield initiation at the coating surface.

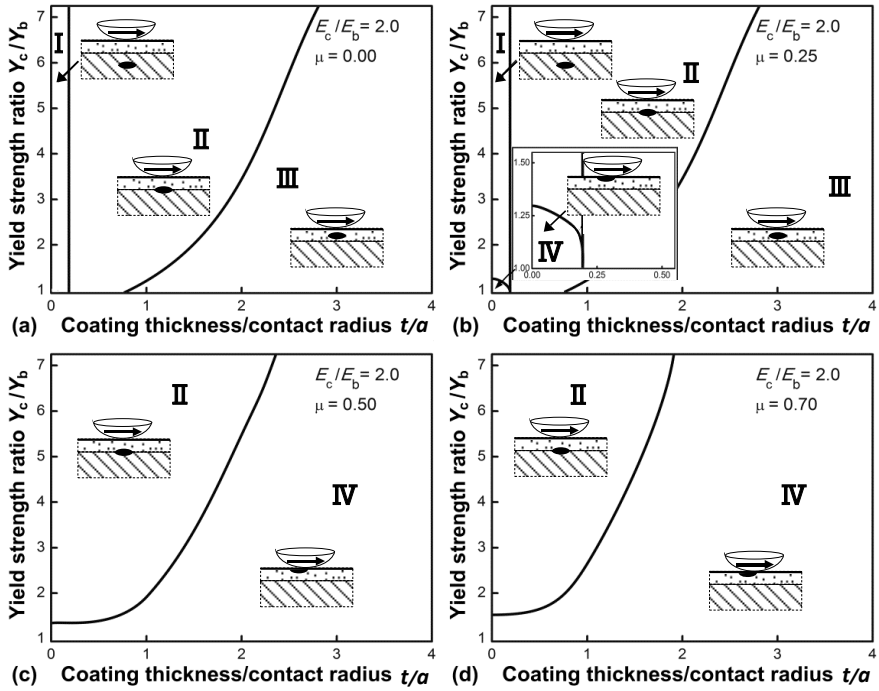

Fig. 11.20. Wear maps showing the crack initiation sites by local yield for delamination of coating. Y_c /Y_b = yield strength of coating / yield strength of substrate, t/a = coating thickness / contact radius. (a) μ = 0.25, (b) μ = 0.25, (c) μ = 0.50, (d) μ = 0.70[16].

When the yield is initiated in the substrate on the region Ⅰ, wear particles similar to those in Fig.11.6 can be generated, and when the yield is initiated at the bonding interface on the region Ⅱ, wear particles similar to those in Fig.11.5 can be generated. The delamination observed in Fig.11.13 can be generated by the yield initiation within the coating on the region Ⅲ. When the yield initiates at the coating surface on the region Ⅳ, the progressive wear observed in Fig.11.4 can be generated in general. Figs.11.20 (a), (b), (c) and (d) are useful in this way to predict the possible wear mode for the given condition of t/a, Y_c/Y_b, E_c/E_b and μ. Therefore, the diagram like ones in Fig.11.20 may be called as "Wear Map of Coating"

11.6 Summary

The mechanisms of delamination wear of hard coatings are described by the theoretical models based on experimental results in nano and micro meter scales. Eqs. (11.1) and (11.2) of critical loads introduced for predicting the generation of ring (Hertz) and lateral cracks in indentation of a hard spherical pin tip are practically useful.

The wear map shown in Fig.11.20 is also useful for predicting wear modes corresponding to the coating thickness and material properties of coating and substrate together with the friction coefficient at the contact interface. Wear maps of this kind are useful for the optimum design of coating by considering the combination of materials, coating thickness, friction coefficient, contact load and shape of contact elements.

It must be noted that the thickness of coating becomes smaller by progressive wear under repeated sliding and as a result the value of t/a (coating thickness / contact radius) is shifted to the side of smaller value of t/a on the maps of Fig.11.20 introducing the transition of wear mode from one to another. It is also important to notice that the contact radius is a function of pin tip radius, elastic moduluses of coating and substrate, load and the shape of wear track formed by the progressive wear.

The wear map shown in Fig.11.20 must be modified when the yield strength at the bonding interface is very different from that of coating or substrate. It can be further modified for better practical use if any new criterion of crack initiation and/or propagation would be introduced in addition to the local yield criterion in the coating, at the bonding interface and in the substrate.

References

[1] K. Holmberg, A. Mattkews, Coatings Tribology, Tribology Series, 28 (Eds D. Dowson et al.), Elsevier, The Netherlands, 1994.

[2] K. Kato, Micro-mechanisms of wear - wear models. Wear, 153 (1992) 277-295.

[3] K. Kato, Microwear mechanics of coating, Surf. Coat.Technol.,76-77(1995) 469-474.

[4] D. F. Diao, K. Kato, K. Hokkirigawa, Fracture mechanisms of ceramic coatings in indentation. Trans. ASME J. Tribology, 116 ,October, (1994) 860-869.

[5] B. R. Lawn, Fracture of Brittle Solids, Cambridge University Press, New York, 1993, pp. 251-256.

[6] B. R. Lawn, A. G. Evans, D. B. Marshall, Elastic/plastic indentation damage in ceramics : The medium/radial crack system. J. Am. Ceram. Soc., 63 (1980) 574-581.

[7] D. B. Marshall, B. R. Lawn, A. G. Erans, Elastic/plastic indentation damage in ceramics : The lateral crack system, J. Am. Soc., 65 (1982) 561-566.

[8] K. Kato, D . F. Diao, M. Tsutsumi, The wear mechanism of ceramic coating film in repeated sliding friction, ASME Wear of Materials, (1991), 243-.248.

[9] D. F. Diao and Y. Sawaki, Fracture mechanisms of ceramic coating during wear, Thin Solid Films, 270 (1995) 1-2, 362-366.
[10] K. Kato, N. Umehara, H. Koide, Micro-wear mechanics of thin hard coating sliding against diamond tip of AFM, Adv. Inf. Stor. Syst., 9 (1997) 289-302.
[11] D. F. Wang, K. Kato, Nano-scale fatigue wear of carbon nitride coatings: Part I − Wear properties, Trans. ASME J. Tribology, 125 (2003) 430-436.
[12] D. F. Wang, K. Kato, Nano-scale fatigue wear of carbon nitride coatings: Part II − Wear mechanisms, Trans. AMSE J. Tribology, 125 (2003) 437-444.
[13] D.Tabor, The hardness of metals, Clarendon Press,(1951).
[14] S. S. Manson, Fatigue: A complex subject-some simple approximations. Exp. Mech., 5 (1965) 193-226.
[15] L. F. Coffin Jr., N. Y. Schenectady, A study of the effects of cyclic thermal stresses on a ductile metal, Trans. ASME, 76 (1954) 931-950.
[16] P. Y. Zhang, D. F. Diao, Z. J. Wang, Three-dimensional local yield maps of hard coating under sliding contact, ASME, Trans, J. Tribology, 134 (2012) 011301-1-8.